

# Dynamical Properties of Charged Stripes in $\text{La}_{2-x}\text{Sr}_x\text{CuO}_4$

L. Tassini,<sup>1</sup> F. Venturini,<sup>1,\*</sup> Q.-M. Zhang,<sup>1,†</sup> R. Hackl,<sup>1</sup> N. Kikugawa,<sup>2,‡</sup> and T. Fujita<sup>2,§</sup>

<sup>1</sup>Walther Meissner Institut, Bayerische Akademie der Wissenschaften, 85748 Garching, Germany

<sup>2</sup>ADSM, Hiroshima University, Higashi-Hiroshima 739-8526, Japan

(Dated: December 2, 2024)

Inelastic light-scattering spectra of underdoped  $\text{La}_{2-x}\text{Sr}_x\text{CuO}_4$  (LSCO) single crystals are presented which provide direct evidence of the formation of one-dimensional charged structures in the two-dimensional  $\text{CuO}_2$  planes. The “stripes” manifest themselves in a Drude-like peak at low energies and temperatures. The selection rules allow to determine the orientation to be along the diagonals at  $x = 0.02$  and along the principle axes at  $x = 0.10$ . The electron-lattice interaction determines the correlation length which turns out to be larger in compound classes with lower superconducting transition temperatures. Temperature is the only scale of the response at different doping levels demonstrating the importance of quantum critical behavior.

PACS numbers: 74.72.-h, 33.20.fb, 74.20.F

Spin-charge separation is a well-known phenomenon in one-dimensional (1D) conductors [1]. It has also been proposed to occur in the essentially two-dimensional (2D) copper-oxygen planes of high-temperature superconductors [2, 3, 4]. Under certain circumstances static charged “stripes” in an antiferromagnetically ordered matrix [5] are observed such as sketched in FIG. 1. The phenomenon can be envisaged as a periodic charge modulation best comparable to an incommensurate density wave. Moreover, there are several scenarios in which charge and spin ordering play a pivotal role in explaining superconductivity [6, 7]. In particular, charge ordering fluctuations would be capable to provide an effective mechanism for the formation of Cooper pairs [6, 8]. Therefore, apart from being an interesting phenomenon in itself the understanding of the dynamics of stripes is an important issue in the cuprates.

In recent years a great variety of methods have been employed to study stripes [8]. In underdoped cuprates regular patterns in the electron distribution can eventually be observed in the pseudogap state [9] by scanning tunneling microscopy [10]. Infrared spectroscopy (IRS) or inelastic light scattering show the *dynamical* behavior particularly well. Strong peaks at low but finite energy develop in the conductivity  $\sigma'(\omega, T)$  and in the Raman response  $\chi''(\omega, T)$  [11, 12, 13]. An explicit calculation demonstrates the existence of an absorption at low-energy due to a transverse excitation of charged stripes [14]. As in the case of IRS the Raman spectra observed in  $\text{La}_{1.90}\text{Sr}_{0.10}\text{CuO}_4$  [12] are similar to those in the ladder compound  $\text{Sr}_{14}\text{Cu}_{24}\text{O}_{41}$  [15, 16]. Therefore, it is qualitatively clear which type of response one can expect in systems with a tendency to form charged 1D stripes.

A crucial test of the interpretation of the Raman spectra in  $\text{La}_{1.90}\text{Sr}_{0.10}\text{CuO}_4$  in terms of fluctuating stripes [12] can be obtained via the selection rules. The response due to charge ordering is expected in the  $B_{1g}$  ( $x^2 - y^2$ ) and in the  $B_{2g}$  ( $xy$ ) symmetry for stripe orien-

tations along the principal axes and the diagonals of the copper-oxygen planes, respectively. LSCO turns out to be an appropriate system for a direct check since the orientation of the stripes depends on doping. It was found by neutron scattering that for  $x_s \simeq 0.055$  the magnetic superstructure rotates from diagonal to parallel [17].

In this Letter, we show that charged stripes can be directly observed in a Raman experiment. The high intensity of the additional response at low doping allows to determine the temperature dependence of fluctuating stripes. The scaling behavior raises implications on quantum criticality in the cuprates.

Standard light scattering equipment was used for the experiments. The electronic Raman response  $\chi''_\mu(\omega, T)$

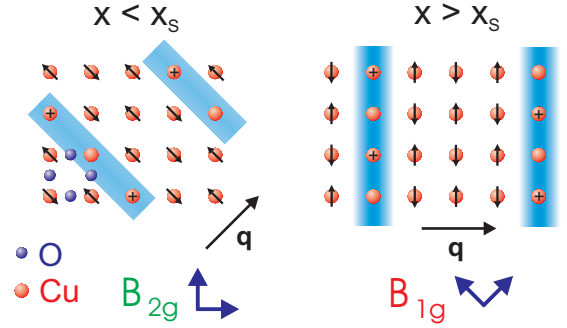


FIG. 1: Sketch of spin-charge-ordered states in the copper-oxygen plane (adopted from ref. [5]). There are antiferromagnetic insulating areas and charged spin-free “stripes”. The modulation is characterized by the vector  $\mathbf{q}$ . If the pattern fluctuates [8] the correlation length  $\xi_s$  is finite and can be as small as a few lattice constants. The response of 1D objects perpendicular to the modulation direction  $\mathbf{q}$  can only be observed by Raman scattering if the polarization vectors of both the incoming and the outgoing photons have a finite projection on either  $\mathbf{q}$  or the stripe direction for transverse or longitudinal excitations, respectively. This implies that stripes parallel to the principal axes can be observed only in  $B_{1g}$  and diagonal ones only in  $B_{2g}$  symmetry.

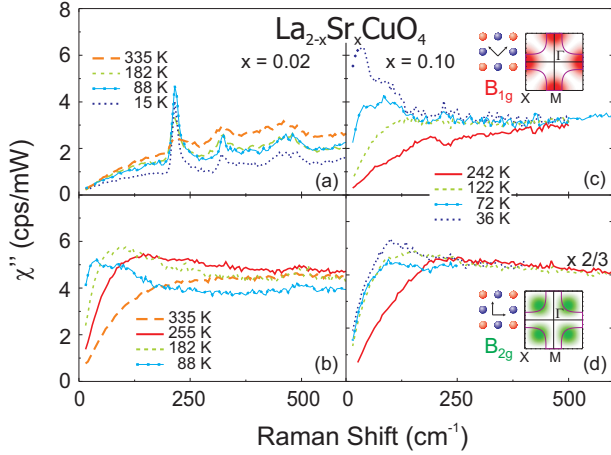


FIG. 2: Raman response  $\chi''(\omega, T)$  of  $\text{La}_{1.98}\text{Sr}_{0.02}\text{CuO}_4$  (a,b) and  $\text{La}_{1.90}\text{Sr}_{0.10}\text{CuO}_4$  (c,d). As indicated in the insets, areas around the M point and the center of the quadrant are projected out in  $B_{1g}$  and  $B_{2g}$  symmetry, respectively, on a quadratic 2D lattice. The selection rules for 1D structures are explained in FIG. 1.

with the symmetry index  $\mu = B_{1g}, B_{2g}$  etc. is a quantity similar to the conductivity  $\sigma'(\omega, T)$ . The symmetries  $\mu$  can be selected by the polarizations of the incident and the scattered photons and correspond to form factors projecting out different electron momenta. Hence, the response is a momentum sensitive transport quantity [18, 19], and the slope of the spectra at  $\omega = 0$ ,  $\tau_0^\mu(T)$ , is proportional to a  $\mathbf{k}$  resolved dc conductivity.

In FIG. 2 the  $B_{1g}$  and  $B_{2g}$  spectra of LSCO at  $x = 0.02$  and  $x = 0.10$  can be compared. At  $x = 0.10$  the  $B_{2g}$  spectra [FIG. 2 (d)] and their temperature dependence are similar to those in Bi-2212 and Y-123 exhibiting an increase of the slopes and hence a decrease of the dc scattering rates (“Raman resistivities”)  $\Gamma_0^{B_{2g}}(T) = \hbar/\tau_0^{B_{2g}}(T)$  upon cooling. For  $B_{1g}$  symmetry [FIG. 2 (c)] the spectra are relatively flat at room temperature while a dramatic increase of the initial slope occurs upon cooling leading to a pile-up of intensity at low energies quite similar to what is found in ladder compounds [16]. At low doping,  $x = 0.02$ , the  $B_{1g}$  behavior [FIG. 2 (a)] expected for this doping level is restored while the initial slope of the  $B_{2g}$  spectra (FIG. 2 b) increases as strongly as that of the  $B_{1g}$  spectra at  $x = 0.10$  [FIG. 2 (c)]. In either symmetry [FIG. 2 (a), (b)] the overall intensity decreases upon cooling indicating a reduction of the number of free carriers as anticipated from the resistivity. For this reason there is no pile-up of the  $B_{2g}$  intensity at  $x = 0.02$ .

For better visualization of the dc behavior we plot in FIG. 3 (aa)–(ad) the temperature dependences of  $\Gamma_0^\mu(T)$  of LSCO. All samples studied are included. At the first glance, no systematic behavior can be found. For  $x \geq 0.10$ ,  $\Gamma_0^{B_{2g}}(T)$  follows the transport [(FIG. 3 (ab)–(ad)] while decreasing rapidly then saturating at  $x = 0.02$

[FIG. 3 (aa)].  $\Gamma_0^{B_{1g}}(T)$  is very similar to  $\Gamma_0^{B_{2g}}(T)$  at  $x = 0.26$  [FIG. 3 (ad)] indicating essentially isotropic electronic properties. For the lower doping levels and high temperatures  $\Gamma_0^{B_{1g}}(T)$  is much larger than  $\Gamma_0^{B_{2g}}(T)$ . Slight and very strong decreases of  $\Gamma_0^{B_{1g}}(T)$  upon cooling are found for  $x = 0.15$  [FIG. 3 (ac)] and  $x = 0.10$  [FIG. 3 (ab)], respectively. For  $x = 0.02$   $\Gamma_0^{B_{1g}}(T)$  [FIG. 3 (aa)] looks weakly insulating showing a similar variation with temperature as the resistivity. However, a direct comparison of resistivity and Raman scattering rates such as at higher doping levels is not possible here since in an essentially insulating sample a Drude-type of relationship between the two quantities does not exist here.

The new features of LSCO are highlighted by comparison with the results in  $\text{Bi}_2\text{Sr}_2\text{CaCu}_2\text{O}_{8+\delta}$  (Bi-2212) and  $\text{YBa}_2\text{Cu}_3\text{O}_{6+x}$  (Y-123). For Bi-2212 the doping dependences of  $\Gamma_0^\mu(T)$  are compiled in Fig. 3 (ba)–(be) (which is partially reproduced from references [20, 21]). Here, a systematic trend is found in both symmetries:  $\Gamma_0^{B_{2g}}(T)$  follows closely the resistivity and  $\Gamma_0^{B_{1g}}(T)$  exhibits increasingly insulating behavior below  $p \simeq 0.22$  [21]. In Y-123 [FIG. 3 (ca)–(cc)] a similar trend is found, even if  $\Gamma_0^{B_{1g}}(T)$  evolves less clearly towards an insulator at low doping. In any case, the strong temperature dependences of  $\Gamma_0^{B_{1g}}(T)$  and  $\Gamma_0^{B_{2g}}(T)$  of LSCO at  $x = 0.10$  and  $x = 0.02$ , respectively, is related to an additional response appearing as a strong peak at low energy and temperature.

This new peak can be separated out to a good approximation by subtracting the “background” of the 2D  $\text{CuO}_2$  planes as expected from Bi-2212, Y-123 or, more directly, from the high-temperature spectra of LSCO. Only the doping levels  $x = 0.02$  and  $x = 0.10$  will be considered since the additional intensity is particularly strong here and details of the subtraction are less important. In order to avoid any additional influence we assume that the 2D response is independent of temperature and is given by the spectra at 335 and 242 K for  $x = 0.02$  and  $x = 0.10$ , respectively. After subtraction, a Drude-like spectrum [22] comparable to the one in  $\text{Sr}_{14}\text{Cu}_{24}\text{O}_{41}$  [16] with a strongly temperature dependent characteristic energy  $\Omega_c(x, T)$  corresponding to the peak position or, equivalently, to the Drude width is obtained [FIG. 4 (a), (b)]. The experimental peaks are somewhat narrower than expected for the Drude response. In spite of the different scattering symmetries at  $x = 0.02$  and  $0.10$  the spectral shapes are remarkably similar if a factor of approximately 2 in the temperature scales is taken into account [compare FIG. 4 (a) and (b)].

In FIG. 5  $\Omega_c(x, T)$  is plotted for the two samples studied. In either case the temperature dependence is similar to that of  $\Gamma_0^\mu(x, T)$  [FIG. 3 (aa) and (ab)] although the magnitude of  $\Omega_c(x, T)$  is smaller by a factor of order 2. Independent of doping,  $\Omega_c(x, T)$  and  $\Gamma_0^\mu(x, T)$  saturate

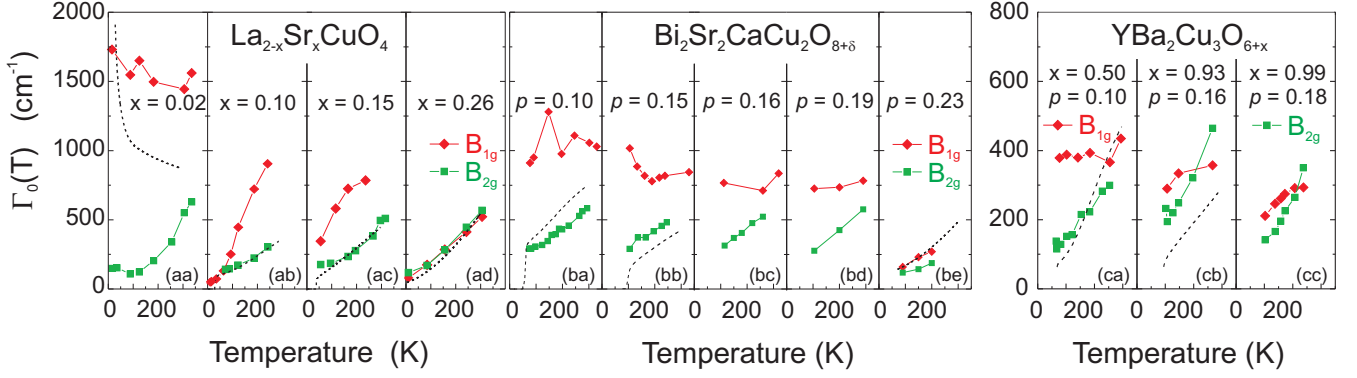


FIG. 3: Static electron relaxation rates  $\Gamma_0^\mu(T)$  of LSCO (aa–ad), Bi-2212 (ba–be), and Y-123 (ca–cc) at various doping levels as measured by Raman scattering. The number  $p$  of holes per  $\text{CuO}_2$  formula unit is equal to  $x$  in LSCO. In Y-123 and Bi-2212  $p$  is a more complicated function of  $x$  and  $\delta$ , respectively. For the relationship between symmetry and sensitivity confere FIG. 2. The dashed lines represent conventional dc resistivities being directly related to  $\Gamma_0^\mu(T)$  in a Drude picture [19].

at low temperature at approximately the same energy of 25–30 and 45–50  $\text{cm}^{-1}$ , respectively. For  $x = 0.02$ ,  $\Omega_c(T)$  and  $\Gamma_0^{B_{2g}}(T)$  are essentially constant below 100 K while the saturation is shifted downwards at  $x = 0.10$ .

At sufficiently high temperature one finds  $\hbar\Omega_c(x, T) \propto k_B T$ . However, the linear parts do not extrapolate to the origin but rather cut the abscissa at doping dependent points  $T^*(x)$ , hence  $\Omega_c(x, T) = \alpha(x)[T - T^*(x)]$ . Similar results for  $T^*(x)$  are obtained on the basis of  $\Gamma_0^\mu(x, T)$  [cf. FIG. 3 (aa) and (ab)]. The results of the

extrapolation are plotted as circles and triangles in inset (a) of FIG. 5. Inset (b) of FIG. 5 explicitly demonstrates the scaling of  $\Omega_c(x, T)$  with temperature. For the two doping levels studied the scaling factor is 2 implying that  $T^*(0.02) \simeq 2T^*(0.10)$ . Since the linear part of both  $\Omega_c(x, T)$  and  $\Gamma_0^\mu(x, T)$  are not very well defined the scaling most likely gives a better estimate of the ratio  $T^*(0.10)/T^*(0.02)$ . For finding the doping level  $x_c$  we extrapolate  $T^*(x)$  obtained by the different methods to zero (inset (a) of FIG. 5).  $T^*(x)$  vanishes for  $0.12 \leq x_c \leq 0.18$ .

The temperature and doping dependences of  $\Omega_c(x, T)$

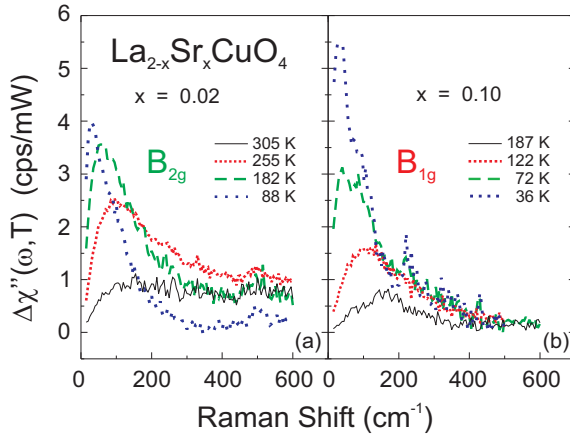


FIG. 4: Response of fluctuating charge order. A Drude-like peak [22] with a characteristic energy  $\Omega_c(x, T)$  is revealed after subtraction of the 2D response of the  $\text{CuO}_2$  planes given by the spectra obtained at the respective highest measuring temperatures (see FIG. 2). At  $x = 0.02$  (a) and  $0.10$  (b) the additional response is observed in  $B_{2g}$  and  $B_{1g}$  symmetry, respectively. The styles of the lines (colours) do not correspond to similar temperatures but rather highlight the *scaling* of the response with temperature: similar spectra are obtained if the temperatures differ by approximately a factor of 2.

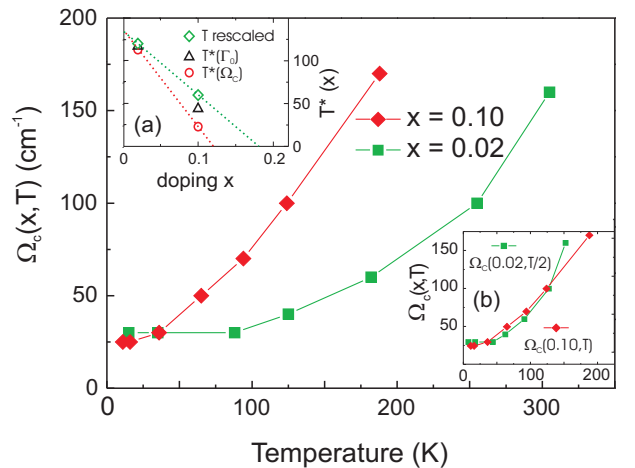


FIG. 5: Temperature dependence of the characteristic energy  $\Omega_c(x, T)$  of the stripe response (see FIG. 4) in LSCO. The approximately linear part at high temperature obeys  $\Omega_c(x, T) = \alpha(x)[T - T^*(x)]$ .  $T^*$  depends on doping and is expected to approach 0 at the quantum critical point (inset a). Inset (b) shows that the temperature is the only scale of  $\Omega_c(x, T)$ . For the two doping levels studied the scaling factor is approximately 2.

and  $T^*(x)$  are reminiscent of a critical line ending in a quantum critical point at  $T = 0$  [23].  $T^*(x)$  should be identified with the pseudogap line [9] within the spread of different value assigned to this quantity by different measurements (for a discussion of the spread of  $T^*(x)$  related to the dynamic nature of the stripes see ref. [23]).  $T^*(x)$  separates a (partially) ordered phase at low temperature from a regime which is dominated by thermal and quantum fluctuations. In this scenario,  $x_c$  is probably better determined by temperature scaling (inset (b) of FIG. 5) but by extrapolating  $\Omega_c(x, T)$  or  $\Gamma_0^\mu(x, T)$  and is close to  $x = 0.18$  rather than 0.12.

The results in LSCO provide direct experimental evidence for the formation of quasi-1D structures at low temperature and doping which can be interpreted in terms of a charge ordering instability. The main support comes from the new type of response [see FIG. 4 (a), (b)] superimposed on the usual spectra of the  $\text{CuO}_2$  planes and its dependence on symmetry demonstrating the re-orientation of the charge modulation as a function of doping as already suggested by neutron scattering on the spin system [17]. At any doping the new response has nothing in common with the dc resistivity [FIG. 3 (aa)] indicating its dynamical and most probably transverse nature.

An important question is why the low-energy response can only be observed in LSCO. It appears that the correlation length  $\xi_s$  of the ordering phenomenon must exceed a minimal value to make the response visible. This corresponds to a fluctuation frequency of order  $\Omega_c \propto (\xi_s)^{-z}$  ( $z = 2$  for damped modes). In the language of quantum phase transitions  $\Omega_c$  can be interpreted as a mass in the fluctuation propagator and is expected to vanish linearly with  $T$  at  $x_c$ . If  $\xi_s$  is substantially smaller than in LSCO  $\Omega_c$  is expected to be larger and the response of the stripes cannot be observed separately from the usual one. This seems to be the case in Bi-2212 and Y-123 at similar doping levels.

We conclude that the charge-ordering instability is an intrinsic feature of the copper-oxygen plane. The maximal doping level up to which the stripes can be observed directly depends on whether or not the lattice helps to stabilize the order. In LSCO  $\xi_s$  has obviously the proper magnitude to allow the observation of the stripes in an optical experiment facilitating a detailed study of the dynamical and critical behavior. If part of the La is substituted by Nd or Eu [5, 24] or if Sr is replaced by Ba [25]  $\xi_s$  increases, and static order is established by a modification of the tilt of the  $\text{CuO}_6$  octahedra or, equivalently, by slightly changing the corrugation of the copper-oxygen plane. Above a critical tilt angle superconductivity is quenched [24]. Apparently, if  $\xi_s$  increases the superconducting transition temperature  $T_c$  decreases suggesting a relation of charge ordering and superconductivity. Since the lattice determines the correlation length  $\xi_s$  it influences  $T_c$  in a subtle, but probably indirect way.

We would like to express our gratitude to L. Benfatto and C. Di Castro for important discussions. The project has been supported by the DFG. F.V. and Q.-M.Z. would like to thank the Gottlieb Daimler - Karl Benz Foundation and the Alexander von Humboldt Foundation, respectively.

- 
- \* Permanent address: Bruker Biospin AG, 8117 Fällanden, Switzerland
  - † Permanent address: National Laboratory of Solid State Microstructures, Department of Physics, Nanjing University, Nanjing 210093, P. R. China
  - ‡ Permanent address: Department of Physics, Kyoto University, Kyoto 606-8502, Japan
  - § Also at: Institute of Spatial Science for Regional and Global Culture, Waseda University, Tokyo 169-8555, Japan
  - [1] J. M. Luttinger, J. Math. Phys. **4**, 1154 (1963).
  - [2] J. Zaanen, O. Gunnarsson, Phys. Rev. B **40**, 7391 (1989).
  - [3] M. Kato, K. Machida, H. Nakanishi, M. Fujita, J. Phys. Soc. Jpn. **59**, 1047 (1990).
  - [4] P. W. Anderson, Phys. Rev. Lett. **67**, 2092 (1991).
  - [5] J. M. Tranquada, B. J. Sternlieb, J. D. Axe, Y. Nakamura, S. Uchida, Nature **375**, 561 (1995).
  - [6] C. Castellani, C. Di Castro, M. Grilli, Z. Phys. B **103**, 137 (1997); C. Castellani, C. Di Castro, M. Grilli, J. Phys. Chem. Solids **59**, 1694 (1998).
  - [7] E. W. Carlson, V. J. Emery, S. A. Kivelson, D. Orgad, *Concepts in High Temperature Superconductivity. In "The Physics of Superconductors"*, Eds. (K. H. Bennemann, J. B. Ketterson, Springer-Verlag, 2004), vol. II, chap. 6, cond-mat/0206217 (2002).
  - [8] For a review and for references see: S. A. Kivelson *et al.*, Rev. Mod. Phys. **75**, 1201 (2003).
  - [9] T. Timusk, B. W. Statt, Rep. Prog. Phys. **62**, 61 (1999).
  - [10] M. Vershinin *et al.*, Science **303**, 1995 (2004).
  - [11] M. Dumm, D. N. Basov, S. Komiya, Y. Abe, Y. Ando, Phys. Rev. Lett. **88**, 147003 (2002).
  - [12] F. Venturini *et al.* Phys. Rev. B **66**, 060502 (2002).
  - [13] A. Lucarelli *et al.*, Phys. Rev. Lett. **90**, 037002 (2003).
  - [14] L. Benfatto, C. Morais-Smith, Phys. Rev. B **68**, 184513 (2003).
  - [15] T. Osafune, N. Motoyama, H. Eisaki, S. Uchida, S. Tajima, Phys. Rev. Lett. **82**, 1313 (1999).
  - [16] A. Gozar *et al.*, Phys. Rev. Lett. **91**, 087401 (2003).
  - [17] S. Wakimoto *et al.*, Phys. Rev. B **60**, 769 (1999); M. Fujita *et al.*, Phys. Rev. B **65**, 064505 (2002).
  - [18] T. P. Devereaux *et al.*, Phys. Rev. Lett. **72**, 396 (1994).
  - [19] T. P. Devereaux, Phys. Rev. B **68**, 094503 (2003).
  - [20] M. Opel *et al.*, Phys. Rev. B **61**, 9752 (2000).
  - [21] F. Venturini *et al.*, Phys. Rev. Lett. **89**, 107003 (2002).
  - [22] A. Zawadowski and M. Cardona, Phys. Rev. B **42**, 10732 (1990).
  - [23] S. Andergassen, S. Caprara, C. Di Castro, M. Grilli, Phys. Rev. Lett. **87**, 056401 (2001).
  - [24] H.-H. Klauss *et al.*, Phys. Rev. Lett. **85**, 4590 (2000).
  - [25] M. Fujita, H. Goka, K. Yamada, and M. Matsuda, Phys. Rev. B **66**, 184503 (2002).